J Eng Math (2008) 60:209–220
DOI 10.1007/s10665-007-9158-2

On the use of conformal mapping for the computation of hydrodynamic forces acting on bodies of arbitrary shape in viscous flow. Part 1: simply connected body

Yves-Marie Scolan · Stéphane Etienne

Received: 8 June 2006 / Accepted: 16 June 2007 / Published online: 24 July 2007

Abstract Some aspects of the force and moment computations in incompressible and viscous flows are revisited. The basic idea was developed in Quartapelle and Napolitano (AIAA J. 21:991–913, 1983). They formulated the way to compute the force and moment without explicitly calculating the pressure. The principle is to project Navier–Stokes equations on a set of functions. Surprisingly these functions have a meaning in potential theory. They are precisely the solutions which give the added masses and added moment of inertia for potential flow. By revisiting this problem for two-dimensional flows in unbounded liquid, a general identity giving the added masses and added moment of inertia is formulated. To this end a conformal-mapping technique is used to transform the fluid domain. Once the potential solution has been obtained, the projection method by Quartapelle and Napolitano is implemented. In addition an a posteriori computation of the pressure is described. Applications illustrate the present study.

Keywords Conformal mappings · Simply connected bodies · Two-dimensional flows

1 Introduction

It is not our intention here to review all the possible formulations of the forces acting on bodies in incompressible and viscous flows. Noca et al. [1] have already written such a review. The present work rather aims to improve an existing formulation. In fact Quartapelle and Napolitano [2] showed how to formulate the force and moment in an integral form without explicitly calculating the pressure. Van der Vegt [3] applied this formulation for viscous flows and more recently Protas et al. [4] and Pan and Chew [5] further developed this approach. Here, subject to the restriction of two-dimensional flows, and thus on the basis of conformal-mapping techniques, the force and moment are formulated. As an intermediate step (see [6]) the calculation of the hydrodynamic-force coefficients in potential theory is revisited. The corresponding boundary-value problem—either formulated for a velocity potential or the stream function—provides a necessary set of variables for the viscous-force calculation. These potentials must be calculated throughout the fluid domain, at least on the vorticity support. The present work offers a generalization of

Y.-M. Scolan (✉)
Ecole Centrale de Marseille, Technopôle Château Gombert, Marseille Cedex 20, 13451, France
e-mail: ymscolan@ec-marseille.fr

S. Etienne
Département de Génie Mécanique, Ecole Polytechnique de Montréal, 2500, Chemin Polytechnique, Montréal, QC, Canada H3T1J4

the theory developed in [5] in the sense that both the force and moment are now formulated. Thus, as an extension of the present method, a way to reconstruct, a posteriori, the pressure pattern is formulated. The asymptotic results in [7] can also be better explained when dealing with oscillating and non-separated flows, that is to say, at low Keulegan–Carpenter number and high Stokes number.

The present work is illustrated by using a Navier–Stokes solver. A Vortex-In-Cell-like model is applied to compute the forces acting on two cross-sections: a square and a loopholed cylinder. The two different force formulations are compared with quite satisfactory agreement.

Part I focuses on a simply connected body. However, the present formulation can be extended to multi-body configurations by using the same approach. Part II will describe corresponding developments.

2 A mathematical solution in potential theory

As a first step the boundary-value problem relative to the potential flow around a moving body is solved. The link with the viscous problem will be given in the next section, but it should be pointed out that the corresponding solutions define a set of test functions for the variational approach developed in [2]. This also gives rise to the force and moment, i.e., the added masses and added moment of inertia. The notations are described in Fig. 1 where the coordinate system $(O, \vec{x}, \vec{y}, \vec{z})$ is direct and attached to the moving body. The normal $\vec{n}$ is directed towards the fluid. The resulting boundary-value problem is classically formulated in terms of the velocity potential ϕ (for unit translational and angular velocities)

$$\begin{cases} \Delta\phi = 0, & \text{in the fluid domain } \Omega, \\ \vec{\nabla}\phi \cdot \vec{n} = \begin{cases} \vec{n} \cdot \vec{x}, \\ \vec{n} \cdot \vec{y}, \\ \vec{n} \cdot (\vec{z} \wedge \vec{r}), \end{cases} & \text{on the body surface } (B), \\ \vec{\nabla}\phi \to 0, & \text{at infinity.} \end{cases} \tag{1}$$

The first two right-hand sides of the Neumann condition on (B) correspond to the calculation of the added masses relative to translational motions in the directions $\vec{x}$ and $\vec{y}$. The third right-hand side gives rise to the added moment of inertia for the rotational motion around the axis $\vec{z}$. More generally the degrees of freedom are numbered $i = 1, 2, 3$ associated with the translations in x (index 1), in y (index 2) and to the rotation (index 3). The matrix of added mass/inertia has thus the coefficients

$$\lambda_{ji} = \rho_f \int_B \phi^{(i)} \phi^{(j)}_{,n} \mathrm{d}\ell, \tag{2}$$

where ρ_f is the density of the fluid. The determination of the coefficients λ_{ij} is obviously not the purpose of this paper. In fact, we are interested in calculating ϕ throughout the fluid domain, not only on the body boundary. There are several standard methods to solve this problem. One of these appears to be the simplest, provided that a conformal transformation of the fluid domain Ω can be determined. As suggested in [8, pp. 328–329], the conformal mapping will map Ω onto the exterior of a unit circle; say $\zeta = \rho \mathrm{e}^{\mathrm{i}\alpha}$ being the image of $Z = x + \mathrm{i}y$ through the mapping as described in Fig. 2. Following [9, Art 9.40], we may conveniently reformulate the boundary-value problem (1) in terms of the stream function ψ. The normal velocity on the moving body is also the tangential derivative of the stream function $\phi_{,n} = \psi_{,s}$ by invoking the Cauchy–Riemann conditions. By integration along the curvilinear coordinate s, it is shown that the stream function satisfies the following Dirichlet boundary-value problem

$$\begin{cases} \Delta\psi = 0, & \text{in the fluid domain } \Omega, \\ \psi = \begin{cases} -y, \\ x, \\ \frac{r^2}{2}, \end{cases} & \text{on the body surface } B, \\ \vec{\nabla}\psi \to 0, & \text{at infinity.} \end{cases} \tag{3}$$

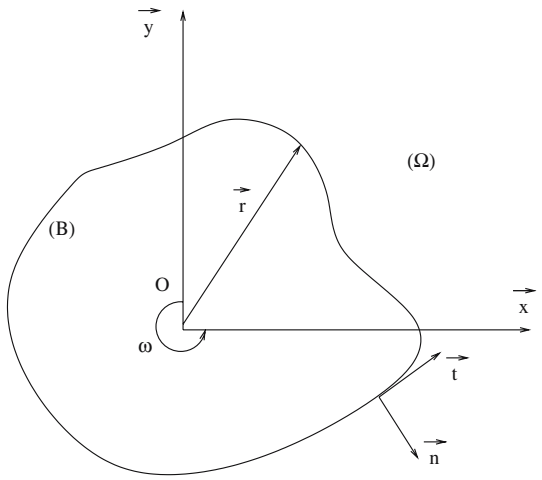

Fig. 1 Coordinates system and notations for the description of the motion of the body (B)

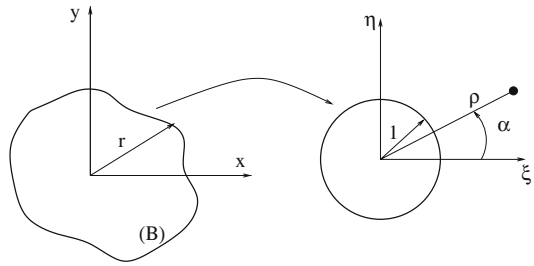

Fig. 2 The physical plane (*left*) is described with the complex number $Z = x + \mathrm{i}y$ and $r = |Z|$; the transformed plane (right) is described with the complex number $\zeta = \xi + \mathrm{i}\eta = \rho \mathrm{e}^{\mathrm{i}\alpha}$; the body contour in the transformed plane is the unit circle through the conformal-mapping function $Z = f(\zeta)$

The flow can be described by a complex potential $F(Z)$ which can be written as

$$F(Z) = \sum_{n=0}^{\infty} \frac{a_n}{\zeta^n}, \tag{4}$$

provided that Z and ζ are mutual images through the conformal-mapping function $Z = f(\zeta)$. The function F has no poles in the fluid domain $|\zeta| > 1$; it is thus analytic throughout the fluid domain. The complex coefficients a_n are unknowns but they will be determined by identifying the Fourier series of x, y and $r^2 = x^2 + y^2$ on (B). Those quantities are simple geometric characteristics of the body shape

$$\left.\begin{array}{l} i = 1, \ -y(\alpha) \\ i = 2, \quad x(\alpha) \\ i = 3, \ \frac{1}{2}r^2(\alpha) \end{array}\right\} = \sum_{n=0}^{\infty} A_n \cos n\alpha + B_n \sin n\alpha, \tag{5}$$

where, for sake of simplicity, the index i does not appear yet in the coefficients (A_n, B_n). The identification of the Fourier coefficients gives $A_n = \Im\mathfrak{m}(a_n)$ and $B_n = -\Re\mathfrak{e}(a_n)$. It follows that the velocity potential ϕ is expressed as

$$\phi = \Re\mathfrak{e}(F) = \sum_{n=0}^{\infty} \frac{1}{\rho^n} \left[A_n \sin n\alpha - B_n \cos n\alpha \right]. \tag{6}$$

The normal along the body contour is written in its complex form

$$n_z(\alpha) = \mathrm{e}^{\mathrm{i}\alpha} \frac{J(\alpha)}{|J(\alpha)|}, \tag{7}$$

where J is the Jacobian $J = \mathrm{d}Z/\mathrm{d}\zeta$ of the transformation. The normal fluid velocity $\phi_{,n}$ can be conveniently turned into

$$\phi_{,n} = \Re\mathfrak{e}\left(\frac{\mathrm{d}F}{\mathrm{d}z} n_z \right) = \frac{1}{|J(\alpha)|} \Re\mathfrak{e}\left(\frac{\mathrm{d}F}{\mathrm{d}\zeta} \mathrm{e}^{\mathrm{i}\alpha} \right). \tag{8}$$

After substituting (4) in (8) and then in (2), the hydrodynamic coefficients simply read

$$\lambda_{ji} = \rho_f \pi \sum_{n=0}^{\infty} n \left(A_n^{(i)} A_n^{(j)} + B_n^{(i)} B_n^{(j)} \right), \tag{9}$$

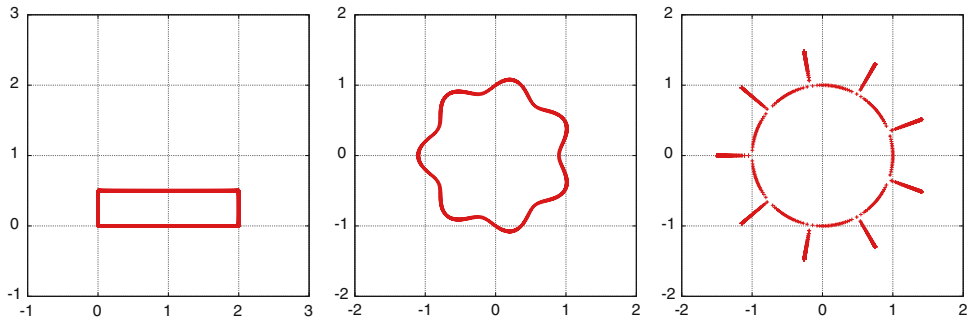

Fig. 3 Three studied shapes: rectangle, section with seven waves and circle with nine fins; the scales in the horizontal direction x and vertical direction y are the same

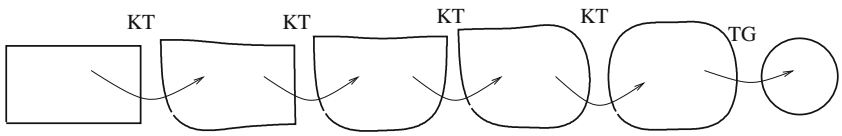

Fig. 4 Successive conformal transformations from a rectangular shape to a unit circle; Theodorsen–Garrick transformation: TG; Karmann–Trefftz transformation: KT

where indices i and j refer to the three possible degrees of freedom. In spite of its evident simplicity, this formula first appeared in [10] and surprisingly, to our knowledge, it never appears in classical textbooks.

These results are illustrated for three shapes in Fig. 3. For a rectangular section the conformal transformations combine successively the Karmann–Trefftz (KT) transformation (see, for example, [11]) which "removes" the corners and then the Theodorsen–Garrick (TG) transformation (see [12]) which turns the intermediate near circle into a perfect circle, as illustrated in Fig. 4. The former transformation can be performed analytically. The latter is more complicated and requires a fixed-point algorithm to calculate the mapping function. More "exotic" shapes can be considered. For a finned circular section, the conformal mapping is described in [13]. It is a succession of simple transformations of analytical form exploiting the cyclic symmetry. The "wavy" section is generated by superimposing a sinusoidal variation of the radius onto a constant radius. This shape is transformed by using a TG transformation; it works as long as the amplitude of oscillation is not too great. So far the amplitude of the oscillations cannot be greater than 10% of the cylinder radius. On the basis of the cyclic symmetry, some improvements of the transformation could be achieved.

For these three shapes the variations of $n(A_n^2 + B_n^2)$ with mode number n are plotted in Figs. 5–7. The rate of decay of the Fourier components clearly depends on the smoothness of the surface. For the finned circle comparisons can be made with exact expressions (see [14, p. 145]) of the added moment of inertia λ_{33} in the restriction of two fins. Figure 8 shows the variations of the non-dimensional mass $\lambda_{22}/(\pi\rho_f R^2)$ and the non-dimensional moment of inertia $\lambda_{33}/(\pi\rho_f R^4)$ (R being the radius of the circle) with the non-dimensional length of the fin a/R. In the present computations, the Fourier series are truncated after 2^9 modes. The relative error for λ_{22} is not larger than 0.08%. The relative error for λ_{33} is calulated with respect to the maximum of λ_{33} over the range $a/R \in [0:1]$; the relative error is less than 0.2%.

3 Force and moment in viscous flows

When dealing with incompressible and viscous flows, we must solve the Navier–Stokes equations formulated here for the velocity $\vec{u}$ and pressure p

$$\vec{u}_{,t} + (\vec{u}\cdot\vec{\nabla})\vec{u} + \frac{1}{\rho_f}\vec{\nabla}p = \nu\Delta\vec{u}, \quad \text{div}\,\vec{u} = 0. \tag{10}$$

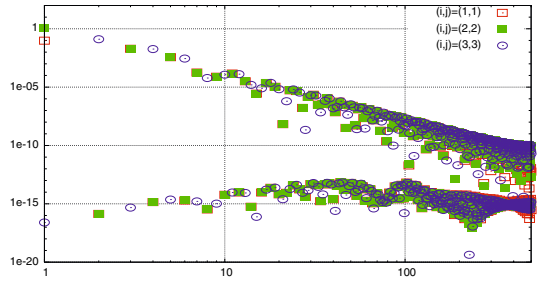

Fig. 5 Rectangular section defined in Fig. 3: variations of $n(A_n^2 + B_n^2)$ with the mode number n

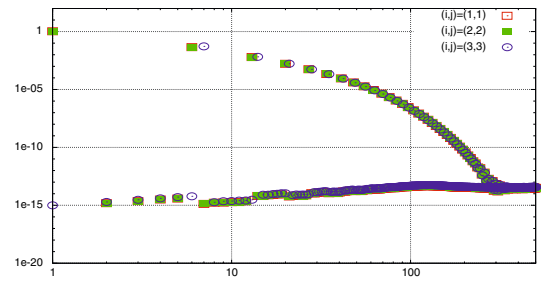

Fig. 6 Wave shape defined in Fig. 3: variations of $n(A_n^2 + B_n^2)$ with the mode number n

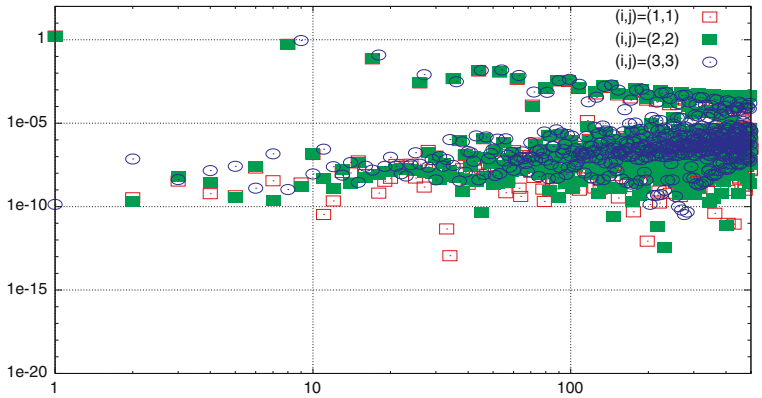

Fig. 7 Finned circle defined in Fig. 3: variations of $n(A_n^2 + B_n^2)$ with the mode number n

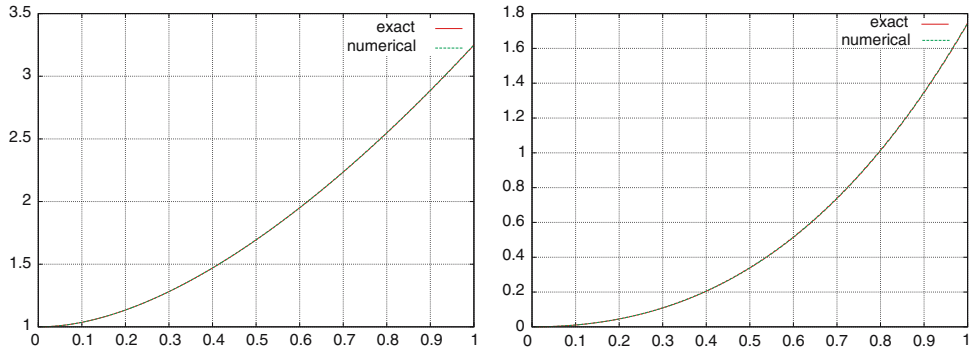

Fig. 8 Circle with two fins: variations of $\frac{\lambda_{22}}{\pi\rho_f R^2}$ (*left*) and $\frac{\lambda_{33}}{\pi\rho_f R^4}$ (*right*) with the length of the fins; comparison of the present formulation (Eq. 9) with the exact results of Newman [14]

For sake of simplicity, the body is now fixed and a no-slip condition is applied on its boundary. The fluid domain extends to infinity. However, the time evolution of the wake is such that it is always possible to confine all of the produced vorticity within a surface of finite size. The stresses acting on the body surface (B) reduce to

$$\vec{\tau} = -p\vec{n} - \rho_f \nu\, (\vec{n} \wedge \vec{\omega}) = -p\vec{n} + \rho_f \nu \omega \vec{t}, \tag{11}$$

where ω denotes the vorticity at the wall. The hydrodynamic forces classically follow from the integration of $\vec{\tau}$

$$\vec{F} = \int_B \vec{\tau}\, \mathrm{d}\ell, \quad \vec{M} = \int_B \vec{r} \wedge \vec{\tau}\, \mathrm{d}\ell, \tag{12}$$

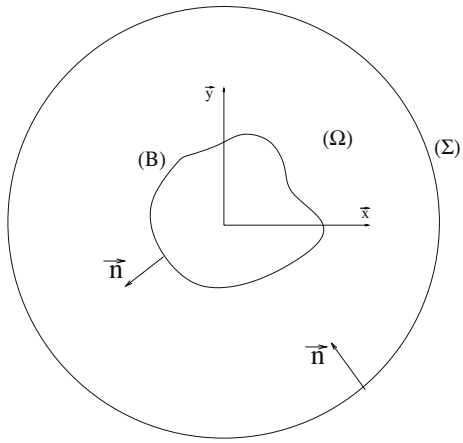

Fig. 9 Sketch of the fluid domain (Ω) bounded with the body contour (B) and a fictitious surface (Σ)

where two contributions are identified either by integrating the pressure or by integrating the friction. These contributions are denoted $(\vec{F}_p, \vec{M}_p)$ and $(\vec{F}_f, \vec{M}_f)$, respectively. In the present context, the moment is calculated with respect to a point O attached to the body. In [2] it is showed how to perform the projection of $\vec{\nabla} p$ on a set of well-chosen functions in order to exhibit the quantities in (12). This requires precisely solving the BVP established in the previous section. After some algebra, one obtains

$$\frac{1}{\rho_f}\int_B p\ \vec{\nabla}\phi\cdot\vec{n}\ \mathrm{d}\ell = -\nu\int_B \vec{\nabla}\phi\cdot(\vec{n}\wedge\vec{\omega})\ \mathrm{d}\ell - \int_\Sigma \phi\ \vec{u}_{,t}\cdot\vec{n}\ \mathrm{d}\ell - \int_\Omega \vec{\nabla}\phi\cdot(\vec{u}\wedge\vec{\omega})\ \mathrm{d}s, \tag{13}$$

where Σ is a contour which surrounds the entire fluid domain as illustrated in Fig. 9. In practice this is a circle with a large radius so that the variables on this contour describe an undisturbed flow. In particular the vorticity ω vanishes on this surface. In the right-hand side of identity (13), three integrals are present. They can be identified as a friction component, an inertial component and a vorticity component. It should be pointed out that the identity (13) is similar whatever the calculated effort (force or moment); this depends on the used $\phi^{(i)}$ among the three possible choices $i \in 1, 2, 3$. In the sequel the three integrals in (13) are noted $I_\nu^{(i)}$, $I_{\mathrm{acc}}^{(i)}$, and $I_\omega^{(i)}$, respectively.

From BVPs (1), ϕ and $\vec{\nabla}\phi\cdot\vec{n}$ are known quantities throughout Ω and on its boundary. In particular, the boundary conditions on B precisely give the normal gradient of ϕ, thus yielding the contribution of the pressure to the hydrodynamic forces and moment

$$\vec{F}_p = \vec{x}\int_B p\ \vec{\nabla}\phi^{(1)}\cdot\vec{n}\ \mathrm{d}\ell + \vec{y}\int_B p\ \vec{\nabla}\phi^{(2)}\cdot\vec{n}\ \mathrm{d}\ell, \tag{14}$$

$$\vec{M}_p\cdot\vec{z} = \int_B p\ \vec{\nabla}\phi^{(3)}\cdot\vec{n}\ \mathrm{d}\ell = \vec{z}\cdot\int_B p\ (\vec{r}\wedge\vec{n})\ \mathrm{d}\ell. \tag{15}$$

It is worth noting that only $\phi^{(3)}$ is calculated from Eq. (6). In fact, it is much simpler to express $(\phi^{(1)}, \phi^{(2)})$ in closed form by using the Circle Theorem. The complex potential F which represents a uniform flow, follows from the formula

$$F(\zeta) = -W_Z^\infty Z + J^\infty W_Z^\infty \zeta + \frac{\overline{J}^\infty \overline{W}_Z^\infty}{\zeta}, \tag{16}$$

provided that $Z = f(\zeta)$. The overline denotes the conjugate of a complex number. In order to obtain the formula (16), we substract the undisturbed potential calculated in the physical plane Z from the total complex potential (expressed in the transformed plane ζ). This presupposes that the body is fixed in an ambient flow and the undisturbed flow can be described by the complex velocity $W_Z^\infty = u_\infty - \mathrm{i}v_\infty$. By definition its conjugate has real and imaginary parts that correspond to the two Cartesian velocity components (u_∞, v_∞) in the physical plane, respectively. It is also related to the complex velocity in the transformed plane through the relation

$$W_Z^\infty = \frac{W_\zeta^\infty}{J^\infty}, \tag{17}$$

where

$$J^{\infty} = \lim_{|z| \longrightarrow \infty} \left(\frac{\mathrm{d}z}{\mathrm{d}\zeta} \right) \tag{18}$$

is the asymptotic expression of the Jacobian J in the far field. This is a complex constant as long as the mapping is conformal and the body is simply connected. This could be properly shown by using the Schwarz–Christoffel integral applied to a closed polygon.

For unit velocity amplitude in (16), the two velocity potentials, as introduced in BVP (1), now read

$$\phi^{(1)} = -x + \mathfrak{Re}\left[J^{\infty}\zeta + \frac{\overline{J}^{\infty}}{\zeta} \right] \tag{19}$$

and

$$\phi^{(2)} = -y + \mathfrak{Im}\left[J^{\infty}\zeta - \frac{\overline{J}^{\infty}}{\zeta} \right], \tag{20}$$

By using the identities (19) and (20), the calculation of the different contributions in (13) will now be given.

3.1 Inertia forces

The body is supposed to be placed in a uniform flow $\vec{v}_{\infty} = u_{\infty}(t)\vec{x} + v_{\infty}(t)\vec{y}$ whose Cartesian components are functions of time only. The dot denotes the time derivative and $(\dot{u}_{\infty}, \dot{v}_{\infty})$ are the Cartesian components of the fluid acceleration in the far field.

It is easily checked that the Jabobian J^{∞} is a constant (not necessarily real) when $|z| \longrightarrow \infty$. We denote this Jabobian by $J^{\infty} = (\mathrm{d}z/\mathrm{d}\zeta)_{\infty}$. This means that we can determine the modification of the orientation of the normal on Σ due to the transformation. Hence, the inner product $(\vec{u}_{,t} \cdot \vec{n})$ reduces to

$$(\vec{u}_{,t} \cdot \vec{n})_z = \dot{u}_{\infty} \cos(\alpha_{\infty} + \alpha) + \dot{v}_{\infty} \sin(\alpha_{\infty} + \alpha), \tag{21}$$

where α_{∞} denotes the argument of the complex variable J^{∞}. The integration in $I^{(i)}_{\mathrm{acc}}$ is then conveniently performed in the ζ-plane. We obtain

$$I^{(i)}_{\mathrm{acc}} = \pi \mathfrak{Re}\left(J^{\infty}(\mathrm{i}A^{(i)}_1 - B^{(i)}_1)(\dot{v}_{\infty} - \mathrm{i}\dot{u}_{\infty}) \right). \tag{22}$$

As an application the ellipse is considered. The semi-axes along the axes (x, y) are noted by (a, b) and the mapping function is $z = f(\zeta) = \frac{1}{2}((a+b)\zeta + (a-b)/\zeta)$. Hence the asymptotic Jacobian is $J^{\infty} = (a+b)/2$. The components $\phi^{(i)}$ and the corresponding $I^{(i)}_{\mathrm{acc}}$ read

$$\begin{cases} \phi^{(1)} = \frac{b\cos\alpha}{\rho} & I^{(1)}_{\mathrm{acc}} = -bJ^{\infty}\pi\dot{u}_{\infty} \\ \phi^{(2)} = \frac{a\sin\alpha}{\rho} & I^{(2)}_{\mathrm{acc}} = -aJ^{\infty}\pi\dot{v}_{\infty} \\ \phi^{(3)} = \frac{1}{4}(a^2+b^2) + \frac{1}{4}(a^2-b^2)\frac{\cos 2\alpha}{\rho^2} & I^{(3)}_{\mathrm{acc}} = 0 \end{cases} \tag{23}$$

The component $I^{(i)}_{\mathrm{acc}}$ cannot be considered as the standard added inertia force. This quantity reduces to the classical added inertia force if and only if the body is circular since $J = 1$ and $a = b = 1$. This aspect makes sense in the light of the following comments regarding the friction forces.

3.2 Friction forces

The formulation in [2] introduces a friction component $I^{(i)}_{v}$. This contribution can be added to the "classical" friction component $(\vec{F}_f, \vec{M}_f)$ yielding a "total" friction force

$$\vec{F}_f + I^{(1)}_{v}\vec{x} + I^{(2)}_{v}\vec{y} = \rho_f \nu \int_B \omega \left(\vec{t} + \phi^{(1)}_{,s}\vec{x} + \phi^{(2)}_{,s}\vec{y} \right) \mathrm{d}\ell, \tag{24}$$

where $\phi^{(i)}_{,s}$ denotes the tangential gradient of $\phi^{(i)}$. After some algebra this total friction force can be written in complex form

$$F_{tf} = 2i\nu J^{\infty} \int_0^{2\pi} \frac{\omega(\zeta)}{|J|^2} \mathrm{e}^{\mathrm{i}\alpha} \mathrm{d}\alpha, \tag{25}$$

where $\omega(\zeta)$ denotes the wall-vorticity in the ζ-plane.[1] This expression is clearly different from that obtained with (11) also written in a complex form

$$F_f = i\nu \int_0^{2\pi} \frac{\omega(\zeta)\mathrm{e}^{\mathrm{i}\alpha}}{\overline{J}(\zeta)} \mathrm{d}\alpha. \tag{26}$$

It should be noted that, reduced to the unit circle (for which $J \equiv 1$ but this remains true for an arbitrary radius), there is a factor 2 between the two expressions (25) and (26). This is quite consistent with the asymptotic analysis by Stokes [15] or Wang [7] who dealt with oscillating flows around a circle. This has been further generalized by Molin and Etienne [16] and Molin [17] for arbitrary shapes. Under the assumptions of low Keulegan–Carpenter number KC and high Stokes number $\beta = \mathrm{Re}/\mathrm{KC}$, it is shown that the friction force plays as significant a role as the pressure force. In the present context and under the same assumptions on the flow, it means that $I^{(i)}_{\omega}$ are of second order. This can be easily checked since the flow is supposed to be unseparated. This means that the domain of integration in $I^{(i)}_{\omega}$ can be reduced to the thickness of the boundary layer, thus varying as $\mathrm{Re}^{-1/2}$. After some algebra it can be shown that the leading term of the integral varies as $\mathrm{Re}^{-3/2}$; hence it is negligible against the friction force.

3.3 "Vorticity" forces

The component of the force containing an integration over the fluid domain can be turned into a more suitable form. This follows from the particular Lagrangian formulation used in the following application of the Vortex-In-Cell method. In fact, a discrete vortex method leads to representation of the vorticity as a set of Dirac masses (denoted δ)

$$\omega(x, y, t) = \sum_{k=1}^{N_v} \Gamma_k \delta(x - x_k)\delta(y - y_k). \tag{27}$$

Each discrete voxtex carries a small amount of circulation Γ_k. This is introduced in the integral $I^{(i)}_{\omega}$ of Eq. (13), thus yielding

$$I^{(1)}_{\omega} = \rho_f \sum_{k=1}^{N_v} \Gamma_k v_k (1 - \mathfrak{Re} B^{(1)}) - u_k \mathfrak{Im} B^{(1)}, \quad \text{with } B^{(1)} = \frac{1}{J}\left[J^{\infty} - \frac{\overline{J}^{\infty}\mathrm{e}^{-2\mathrm{i}\alpha}}{\rho^2}\right], \tag{28}$$

$$I^{(2)}_{\omega} = \rho_f \sum_{k=1}^{N_v} \Gamma_k u_k (\mathfrak{Re} B^{(2)} - 1) - v_k \mathfrak{Im} B^{(2)}, \quad \text{with } B^{(2)} = \frac{1}{J}\left[J^{\infty} + \frac{\overline{J}^{\infty}\mathrm{e}^{-2\mathrm{i}\alpha}}{\rho^2}\right], \tag{29}$$

where u_k and v_k are the Cartesian components of the velocity in the physical plane Z at the vortex number k. These velocity components are actually not directly computed in the present VIC model. In fact, the Poisson equation $\Delta\psi = -\omega$ is solved in the transformed plane. This means that the derivatives in the Laplacian operator are performed with respect to the coordinates attached to the transformed plane. Hence the right-hand side follows from the vorticity distribution in the transformed plane as well. By using the identity $\vec{u} = \vec{\mathrm{rot}}\,\psi\,\vec{z}$, where the curl operator implies derivatives in the transformed plane, we obtain the velocity in this plane ζ and we note it in its complex

[1] The vorticity calculated in the ζ-plane differs from the vorticity calculated in the Z-plane with a factor $|J|^2$, say $\omega(\zeta) = |J|^2\omega(Z)$ since locally the circulation of a discrete vortex would be the same in the two planes.

form W_ζ. The complex velocities in the two planes Z and ζ are then calculated at the vortex point and they are related as follows

$$W_Z = u_k - \mathrm{i}v_k = \frac{W_\zeta^{(k)}}{J}. \tag{30}$$

On the other hand, we have to evaluate the gradient of the ith component $F^{(i)}$ of the complex potential defined in (4), resulting in the following relation

$$\phi_{,x}^{(i)} - i\phi_{,y}^{(i)} = \frac{\mathrm{d}F^{(i)}}{\mathrm{d}\zeta}\frac{1}{J}. \tag{31}$$

Combining (30) and (31), we see that the two-dimensional restriction of $\vec{\nabla}\phi \wedge \vec{u}$ means that the quantities $I_\omega^{(i)}$ can be reduced to

$$I_\omega^{(i)} = -\rho_f \sum_{k=1}^{N_v} \frac{\Gamma_k}{|J|^2} \Im\mathfrak{m}\left[\overline{W}_\zeta^{(k)} \frac{\mathrm{d}F^{(i)}}{\mathrm{d}\zeta}\right]. \tag{32}$$

3.4 Pressure calculation

The usual way to compute the pressure consists in solving a Poisson equation. This equation is obtained by taking the divergence of (10). An alternative for two-dimensional flow follows from the projection of (10) along the tangential direction $\vec{t}$. Then the tangential derivative of the pressure is proportional to the normal derivative of the vorticity

$$\vec{\nabla} p \cdot \vec{t} = \rho_f \nu \vec{\nabla}\omega \cdot \vec{n}. \tag{33}$$

The latter quantity is itself proportional to the time rate of circulation introduced in the fluid at the boundary. This is undoubtedly the easiest way to compute the pressure.

Consistently with the formulation in [2], it is possible to recompute the pressure from the integral form (13). To that end a new set of test functions ϕ must be introduced. To avoid confusion, these functions are now denoted by η and they satisfy the following two BVP:

$$\begin{cases} \Delta\eta = 0, & \text{in the fluid domain } \Omega, \\ \vec{\nabla}\eta \cdot \vec{n} = \frac{1}{|J|} \begin{cases} \cos m\alpha, \\ \sin m\alpha, \end{cases} & \text{on the body surface } (B), \\ \vec{\nabla}\eta \to 0, & \text{at infinity.} \end{cases} \tag{34}$$

where m is an arbitrary positive integer and α is the argument of $\zeta = f^{-1}(z)$ where the complex coordinate z describes the physical contour (B). Knowing the complex normal n_z on (B) from (7), it is easy to show that the possible two solutions are

$$\begin{Bmatrix} \eta^{(1)} \\ \eta^{(2)} \end{Bmatrix} = -\frac{1}{m\rho^m} \begin{Bmatrix} \cos m\alpha \\ \sin m\alpha \end{Bmatrix}. \tag{35}$$

Then the Fourier series of the pressure on (B) is performed in the transformed plane

$$p(\alpha) = \sum_{n=0}^{\infty} C_n \cos n\alpha + D_n \sin n\alpha, \tag{36}$$

thus yielding, by using (13),

$$\frac{\pi}{\rho_f} C_m = \nu \int_0^{2\pi} \frac{\omega_\zeta \sin m\alpha}{|J|^2} \mathrm{d}\alpha - \sum_{l=1}^{N_v} \Gamma_l \left(u_x \eta_{,y}^{(1)} - u_y \eta_{,x}^{(1)}\right), \tag{37}$$

$$\frac{\pi}{\rho_f} D_m = -\nu \int_0^{2\pi} \frac{\omega_\zeta \cos m\alpha}{|J|^2} \mathrm{d}\alpha - \sum_{l=1}^{N_v} \Gamma_l \left(u_x \eta_{,y}^{(2)} - u_y \eta_{,x}^{(2)}\right), \tag{38}$$

where $\vec{\nabla}\eta$ are determined from (35). Alternatively, a more compact form can be written as shown in Sect. 3.3.

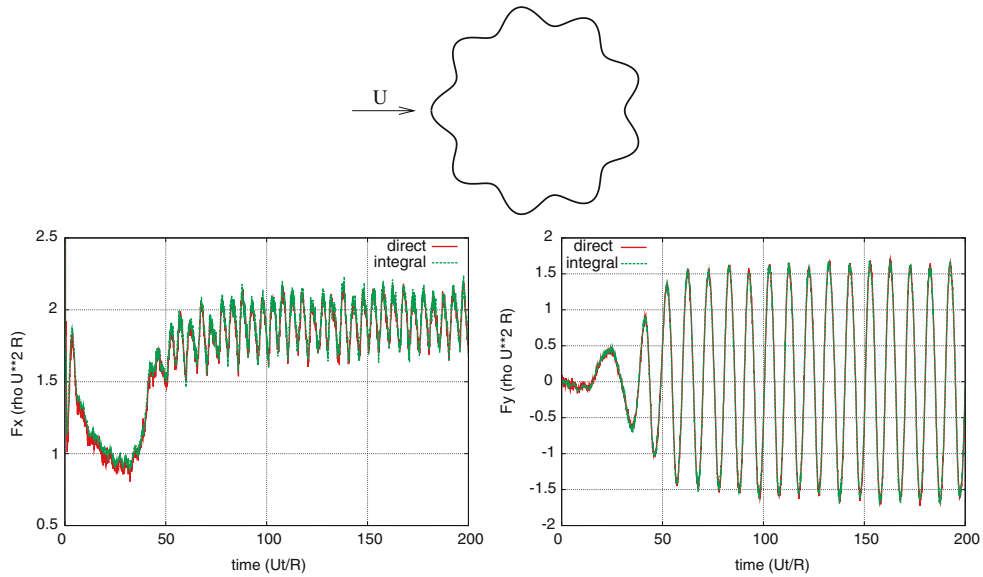

Fig. 10 Circular section of radius R with nine waves of amplitude $a/R = 0.1$ at $\mathrm{Re} = \frac{2RU}{\nu} = 500$: time histories of the force components F_x and F_y following from the two formulations; the force are made non-dimensional with $\rho_f U^2 R$

4 Some illustrative results

In order to solve the Navier–Stokes equations (10), a Vortex-In-Cell model is used (see [18]). The vorticity field is represented by means of discrete vortices. They are generated on the body surface in order to impose a no-slip condition there. Then they are tracked in the flow by using an operator-splitting technique. The diffusion is modelled with a random-walk scheme. The time stepping for the convection is solved by using a second order Runge–Kutta algorithm. The velocity is evaluated by solving a Poisson equation for the stream function with the vorticity as a source term. This vorticity field follows from distributing the circulation of each discrete vortex on a regular mesh. This mesh is generated by the conformal mapping and in the present context where the body contour is turned into a unit circle, the computational domain is an annulus. That makes it possible to decompose the variables as a Fourier series of the polar angle. The remaining partial differential equation in the radial direction is solved by using a second order finite-difference method.

Two formulations of the force are compared. On the one hand, the classical integration of the Cauchy stress tensor is performed. The pressure is thus required. It is calculated by integrating its tangential gradient (Eq. 33) along the body contour. On the other hand, the pressure is not explicitly calculated and the force follows from Eq. 13 to which the standard friction force is added.

Two configurations are studied. The first is a "wavy" contour in a uniform current U and Reynolds number $\mathrm{Re} = 500$. Figure 10 shows the time variation of the force components inline and transverse to the current. Discrepancies between the two formulations are not noticeable with regard either to the amplitude or to the phase. The time variation of the pressure at two points of the contour is plotted in Fig. 11. In the direct approach, the pressure is formulated as in [19], from the normal gradient of parietal vorticity, that is to say, in terms of the rate of circulation per time step (Eq. 33). The integral approach follows from Eqs. 36 to 38. The agreement between the two pressure formulations is satisfactory.

For any shapes with sharp edges, there still remain some numerical difficulties in the present approach. It is known that the derivative of the mapping function (noted here $J = \mathrm{d}z/\mathrm{d}\zeta$) vanishes close to sharp corners. A treatment of J^{-1} is necessary and usually it consists in an artificial cut-off as described in [19]. In spite of the difficulties the agreement is satisfactory. This is illustrated in Fig. 12 where the time variation of the force components inline and

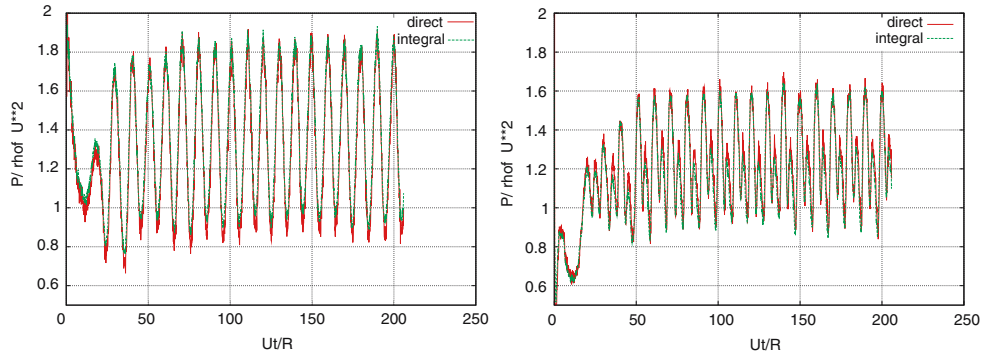

Fig. 11 Circular section of radius R with nine waves of amplitude $a/R = 0.1$ at Re $= \frac{2RU}{\nu} = 500$: time histories of the pressure at location $\alpha = -\pi/2$ and $\alpha = 0$. Direct and integral formulations; the pressure is made non-dimensional with $\rho_f U^2$

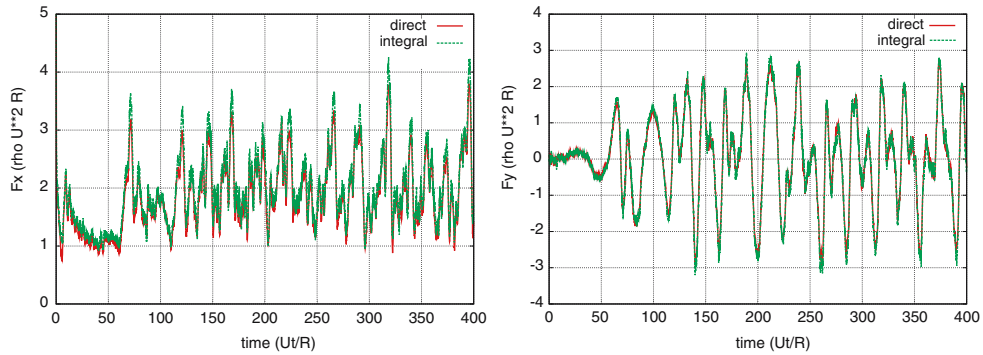

Fig. 12 Square section with length $2R$: time histories of the force components F_x and F_y following from the two formulations; the force are made non-dimensional with $\rho_f U^2 R$

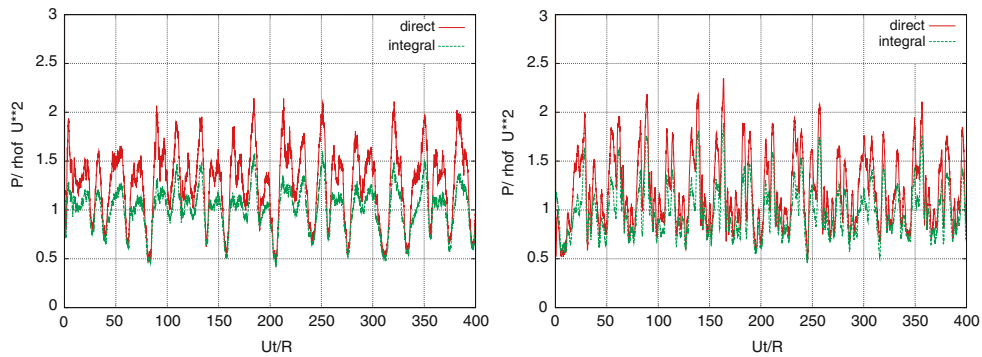

Fig. 13 Square section with length $2R$: time histories of the pressure at location $\alpha = -\pi/2$ and $\alpha = 0$. Direct and integral formulations; the pressure is made non-dimensional with $\rho_f U^2$

transverse with the current for a square in a uniform current at Reynolds Re $= 1{,}000$ is shown. In Fig. 13, the time variation of the pressure at two points of the contour is plotted. The discrepancies originate from the numerical difficulties associated with the inverse Jacobian $1/|J|^2$ that appears in (37) and (38).

5 Conclusion

We have examined two of the various formulations of the viscous forces acting on a two-dimensional body. It appears that, using conformal mapping of the fluid domain onto the exterior of a unit circle, some gain can be expected. Two applications are considered: (1) a smooth body like a circle with a sinusoidal variation of its radius and (2) a shape with sharp edges like a square. The two formulations compare well.

One of the formulations follows from the theoretical developments in [2]. In this formulation, the pressure is not explicitly calculated. It can, in fact, be calculated a posteriori. The pressure contribution in the force is evaluated by projecting the Navier–Stokes equations onto a set of functions. Curiously, these functions have a physical meaning and use in potential theory. This is why some improvements of the velocity-potential calculation around a body in translation and rotation are proposed here. The opportunity is thus offered to provide a surprisingly very simple expression of the added masses and added moment of inertia.

References

1. Noca F, Shiels D, Jeon D (1999) A comparison of methods for evaluating time-dependent fluid dynamic forces on bodies, using only velocity fields and their derivatives. J Fluids Struct 13(5):551–661
2. Quartapelle L, Napolitano M (1983) Force and moment in incompressible flows. AIAA J 21:911–913
3. Van der Vegt JJW (1988) A variationnally optimized vortex tracing algorithm for three–dimensional flows around solid bodies. PhD thesis of the Technische Universiteit Delft
4. Protas B, Styczek A, Nowakowski A (2000) An effective approach to computation of forces in viscous incompressible flows. J Comput Phys 159(2):231–245
5. Pan LS, Chew YT (2002) A general formula for calculating forces on a 2-d arbitrary body in incompressible flow. J Fluids Struct 16(1):71–82
6. Scolan Y-M (2005) Some aspects of the potential flow around rotating bodies. Comptes Rendus Mecanique 333(6):487–492
7. Wang CY (1968) On high-frequency oscillating viscous flows. J Fluid Mech 32:55–68
8. Kochin NE, Kibel IA, Roze NV (1964) Theoretical hydromechanics. Intersciences Publishers
9. Milne-Thomson LM (1960) Theoretical hydrodynamics, 4th edn. McMillan & Co Ltd, New-York
10. Wendel K (1950) Hydrodynamische Massen und Hydrodynamische Massenträgheitsmomente (english translation: 1956). Jahrb. D. STG 44
11. Halsey N (1979) Potential flow analysis of multielement airfoils using conformal mapping. AIAA J 17:1281–1288
12. Theodorsen T, Garrick IE (1933) General potential theory of arbitrary wing sections. NACA Rept 452:177–209
13. Lavrentyev M, Shabat B (1977) Méthodes de la théorie des fonctions d'une variable complexe. Edition du MIR (in French), Moscow
14. Newman JN (1977) Marine hydrodynamics. MIT Press, Cambridge
15. Stokes GG (1851) On the effect of the internal friction of fluids on the motion of pendulums. Trans Cambridge Phil 9:8–106
16. Molin B, Etienne S (2000) On viscous forces on non-circular cylinders in low KC oscillatory flows. Euro J Mech B/Fluid 19(3):453–457
17. Molin B (2004) On the frictional damping in roll of ship sections. Int Shipbuild Progr 51(1):59–85
18. Smith PA, Stansby PK (1988) Impulsively started flow around a circular cylinder by the vortex method. J Fluid Mech 194:45–77
19. Scolan Y-M, Faltinsen O (1994) Numerical studies of separated flow from bodies with sharp corners by the Vortex-In-Cell Method. J Fluid Struct 8:201–230